Overview, comparison, and extension of emergency controls against voltage instability using Inverter-Based Generators

P. Mandoulidis[1], G. Chaspierre[2], C. Vournas[1] and T. Van Cutsem[2]

[1] *School of Electrical and Computer Eng., National Technical University of Athens Greece*

[2] *Department of Electrical Engineering and Computer Science, University of Liège, Belgium*
(Tel: +30-210-7723598; Fax: +30-210-7723659; e-mail: pmandou@power.ece.ntua.gr.

Abstract: This paper provides a general overview of some previously reported schemes for the on-line detection and corrective emergency control of long-term voltage instability in a power system with a significant share of Inverter-Based Generators (IBGs) connected at the distribution level. Next, it proceeds to introduce new wide-area emergency controls to avoid an imminent voltage instability. Reactive support from IBGs is utilized as part of voltage stability emergency control, while in normal operation IBGs are operating at unity power factor. Results are shown for the IEEE Nordic Test System with increased IBG penetration, through feeders adapted from Hellenic Interconnected System wind farms. The newly proposed wide-area controls are compared with existing local emergency control schemes and are shown to have superior performance.

Keywords: Inverter-based generation, long-term voltage stability, stability monitoring, emergency control, load tap changers, reactive support.

1   INTRODUCTION

The proliferation of Inverter Based Generators (IBG) in the distribution grids has caused concerns over recent years about their effect on system dynamics and stability [1]. On the other hand, the control capabilities of IBGs can be a new source of stabilizing actions for the bulk power system, thus they can also offer a new control potential [2]. Currently most IBGs operate normally at Unity Power Factor (UPF), but several other options are technically possible, such as local voltage control, or reactive power injection control, subject always to constraints set by converter rating, as well as by distribution voltage acceptable limits, as set be grid codes. An alternative coordinated control configuration is suggested in [3], where distribution voltage is regulated by the IBGs while Load Tap Changers (LTC) of the feeding transformers are maintaining the reactive capability margin of the IBGs. An extensive review on the voltage control opportunities in smart grids is provided in [4]. A recent investigation focusing on the effect of IBGs on voltage stability is presented in [5], showing increase of voltage stability margins when IBGs are connected into the grid and operate under various control schemes. Similar results showing increased stability margins with IBGs connected at the distribution level were reported in [6] where both UPF and voltage control modes were considered for converter control. Other research efforts, such as in [7], focus on the operational efficiency of active distribution networks, with a view to enhance security, mitigate operational costs and maximize the IBG penetration potential within an active distribution network. Thus, IBGs constitute both a challenge and an opportunity for voltage stability.

This paper goes one step beyond voltage and reactive power control of the distribution feeder under normal operating conditions and focuses on voltage stability emergency control that can be offered by IBGs when needed, subject always to respecting distribution feeder constraints. Prior research on reactive support by the IBGs, combined with modified Load Tap Changer (LTC) control, in order to support transmission voltages during emergencies is reported in [6] and [8]-[10]. This paper reviews and compares existing instability detection and emergency control techniques to avoid an incipient

voltage collapse, and proposes new emergency control schemes with improved performance, as will be discussed later.

The first step for the application of emergency controls against voltage collapse is the detection of incipient voltage instability through measurements in real time. Measurement-based, real-time, voltage stability monitoring is a theme of growing interest due to the extending deployment of Phasor Measurement Units (PMU) in power systems, as well as to the increasing complexity added by the proliferation of IBGs. A survey of voltage instability detection methods was presented in [11]. Several voltage stability monitoring approaches are also shortly reviewed in [12]. A critical appraisal of older and newer monitoring techniques based on the concept of impedance matching, as well as a newly developed technique to overcome critical issues, can be found in [13]. Another voltage stability monitoring approach has been applied to the Nordic Power Operations Center and is reported in [14]. An agent-based voltage stability identification method is reported in [15] and an adaptation of the impedance matching approach is reported in [16]. For the existing emergency control schemes reviewed in this paper, monitoring of long-term voltage instability is performed using the LIVES method [17]-[19], which is based on LTCs of bulk power delivery substation transformers. Alternatively, the New LIVES Index (NLI) introduced in [20], which uses substation PMU measurements installed in the EHV network, is introduced as alarm/reset criterion for a new, wide-area, emergency control scheme, able to operate in closed loop.

The methods for voltage instability emergency control can be classified into two broad categories, according to whether they resort to measurements gathered at one location, or they are using wide-area monitoring and control. Local emergency controls do not require communication outside the distribution substation and feeder, since voltage measurements at transmission and distribution substation buses are available locally. The only communication needed is for emergency signals to be sent to the IBGs initiating, or terminating, their reactive support. Wide-area control schemes, on the other hand, use the alarm issued at different locations to simultaneously initiate corrective actions in all substations and feeders within a pre-specified area, and start/stop those actions, based on measurements collected at transmission buses. Clearly, further communication infrastructure is necessary to implement wide-area control schemes. Combinations of local and wide-area schemes are also possible. The previously developed emergency controls reviewed in this paper are local ones, while the newly proposed control schemes are of the wide-area type.

In all cases, when IBG reactive support is required, this is provided respecting local feeder voltage limits at their specified values (typically $\pm5\%$), as well as maximum current capability of the converter, which in this paper is taken equal to the rated value. A major problem when designing voltage stability emergency controls involving IBGs connected to the same distribution feeder with voltage sensitive loads [8],[9] is the interaction between the load restoration affected indirectly through voltage recovery, and the reactive support offered by IBGs. Since the voltage of the feeder is regulated by the LTC of the distribution transformer, the coordination between LTC emergency control (e.g. voltage setpoint adjustment) and the reactive support from IBGs is a major part of the control schemes compared in this paper. In particular, fast voltage rise at distribution level due to IBG reactive injection can be detrimental during emergencies, as it results (transiently, i.e. before the LTC has time to correct the voltage rise) in higher load consumption. Thus, the required reactive support from IBGs has to be limited in its ramp rate, so that LTCs can maintain the load voltage at the desired value during the IBG reactive support run. The main purpose of the proposed voltage stability emergency control schemes in this paper is to combine the benefits of wide-area IBG emergency reactive support with LTC emergency action and thus provide generic guidelines for this type of control.

The voltage stability emergency control schemes reviewed and presented in this paper are all capable of avoiding an impending voltage collapse, but at different costs. Thus, two metrics are employed

as basis for their comparison: a) the amount of indirectly reduced load consumption to achieve stabilization and b) the remaining reserve on IBGs for further reactive support. All approaches, old and new, are tested and compared on the fully documented IEEE Nordic Test System [21]. This system was already augmented in [6],[8] to include a significant proportion of IBGs connected at the distribution level of the Central Area, without altering the initial power flow of the insecure operating point A documented in [21], by appropriately scaling up initial loads.

The main contributions of this paper can be summarized in the following:

- Extension of IBG emergency control schemes aimed at protecting against voltage instability
- Utilization of effective and adaptive voltage instability detection methods for emergency protection scheme activation
- Comparison and performance evaluation based on objective criteria.

The rest of the paper is organized as follows. In Section 2 a brief recap of the utilized local voltage instability methods is given, while in Section 3 a description of the existing local voltage instability protection schemes previously proposed by the authors (i.e. Schemes A & B) is presented. Section 4 discusses the functionality and main characteristics of the new global emergency control schemes against long-term voltage instability, whereas in Section 5 the performance criteria of the emergency control schemes are defined, in order to quantify each scheme's performance in an objective way. Section 6 describes the IEEE Nordic Test System and the applied modifications that took place in order to assess the emergency control schemes' performance. The initial operating point A, as described in [21], as well as the performance of the utilized instability monitoring methods on identifying the instability onset is shown. In Section 7, individual results for each emergency control scheme, as well as comparisons are presented, illustrating the benefits as well as the shortcomings of each emergency control scheme. Finally, Section 8 sums up the main conclusions and provides guidelines for practical implementations.

2 ON-LINE VOLTAGE STABILITY MONITORING

In this section a brief description of the on-line measurement-based methods for voltage instability detection used in this paper is briefly summarized for ease of the reader.

2.1 LIVES-Alarm monitoring

Local Identification of Voltage Emergency Situations (LIVES) is a local voltage stability monitoring scheme, originally proposed in [17], which, as shown in [19], can timely and efficiently identify system-wide long-term voltage instability using purely local measurements, namely through the monitoring of the LTC controlled voltages. More specifically, an unstable LTC operation is identified when the distribution voltage at the secondary side of a step-down power transformer fails to increase between two successive LTC actions, indicating violation of the sufficient stability condition described in [17]. During monitoring, the moving average value of the distribution voltage is calculated for a time equal to a single LTC period of operation.

A modified version of the algorithm, namely eLIVES, does not rely on individual LTC operating periods and is able to track the distribution voltage trend by performing recursive least square fitting on the measurements. Originally presented in [18] this algorithm has also proven its efficiency in [15] when utilized in a distributed agent-based scheme with limited communication requirements, thus also leading to an integrated protection scheme against voltage collapse.

The concept of LIVES algorithm relies on the LTC operation and is applied locally at bulk power delivery transformers, i.e. very close to transmission system loads. Since it is directly monitoring stability of load restoration through the effectiveness of distribution voltage control, it is a secure and reliable means to activate emergency controls, which is an advantage over other measurement-based protection and emergency control schemes, based on undervoltage, such as undervoltage load shedding (UVLS). The latter usually requires extensive offline studies to determine voltage thresholds that are both reliable and secure.

2.2 NLI Voltage Stability monitoring

The monitoring of voltage instability through the LIVES concept is not necessarily limited to power delivery substations hosting LTC transformers, but it can be generalized for application in the transmission system. In this respect, the New LIVES Index (NLI) [20] is a generalization of LIVES algorithm based on phasor measurements provided by PMUs installed at transmission buses located at the receiving ends of transmission corridors.

In Fig. 1 a transmission corridor between two areas, an importing area A (assumed prone to voltage instability) and an exporting system area B, are depicted. NLI can be applied on any boundary bus independently. Boundary buses of the importing area A are numbered 1 through n and are shown with red colour. Boundary buses of the exporting area B are shown in green colour. In Area B, k is any bus in the set K_i of exporting boundary buses connected to bus i.
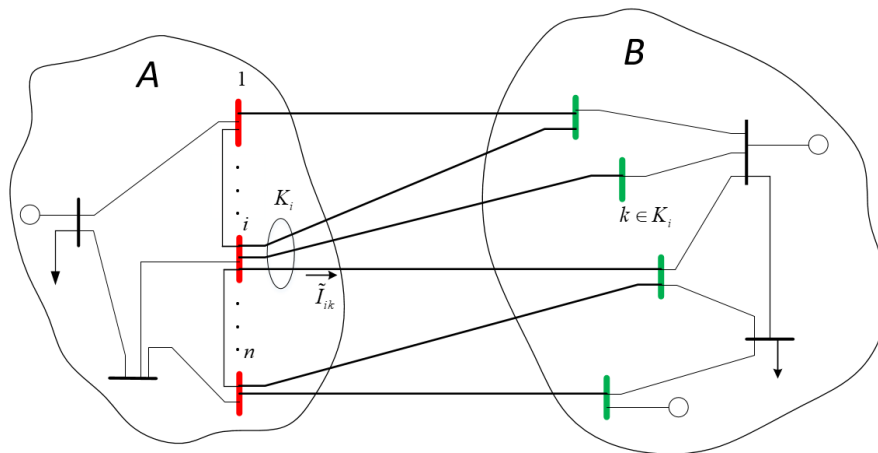

Fig. 1 Transmission system corridor: exporting area B, importing area A.

The index is a metric for long-term voltage instability and is calculated independently for each transmission bus equipped with PMUs providing current and voltage phasor measurements. First, for the boundary receiving bus i in Fig. 1 the incoming current $\overline{I}_i$, i.e. the sum of received currents in the corridor transmission lines incident to bus i is defined as:

$$\overline{I}_i = -\sum_{k \in K_i} \overline{I}_{ik} \tag{1}$$

where the set K_i contains the indices of the sending boundary buses connected to the receiving boundary bus i.

Once $\overline{I}_i$ is defined, NLI at bus i can be calculated according to the following formula:

$$NLI_i = \frac{\Delta P_{r,i}}{\Delta G_i} \qquad (2)$$

where Δ denotes variation between two successive time instants, $\boldsymbol{P_{r,i}}$ is the received active power (i.e. the incoming active power through the corridor transmission lines incident to bus $\boldsymbol{i}$), i.e.:

$$\boldsymbol{P_{r,i}} = \boldsymbol{Re}\{\overline{V_i}\overline{I_i^*}\} \qquad (3)$$

and $\boldsymbol{G_i}$ is the apparent conductance as seen from bus $\boldsymbol{i}$, i.e.:

$$\boldsymbol{G_i} = \boldsymbol{Re}\left\{\frac{\overline{I_i}}{\overline{V_i}}\right\} \qquad (4)$$

Alternatively, NLI can be calculated for every sending boundary bus, the mere difference in the calculations being the total (sending) current calculated as in (1) but without the minus sign. In this case, $\boldsymbol{P_{r,i}}$ has to be replaced by $\boldsymbol{P_{s,i}}$, the total active power sent, and the apparent conductance G_i now involves also the corridor circuits of sending boundary bus i. It is mentioned however, that since $\boldsymbol{P_{s,i}}$ contains in addition the corridor line losses it makes more sense to monitor the NLIs of the receiving boundary buses for better performance.

Similarly to LIVES, a positive NLI implies that load active power is increased when load demand is increased, as shown by positive ΔG. A negative NLI results in an alarm signifying that load power can no longer be restored, thus the voltage stability limit is very close.

The filtering and averaging necessary to obtain long-term trends of power and conductance is detailed in [20]. One important point is that NLI is calculated only when the measured conductance is increasing, as this reflects an increase in load demand and thus system stress. Also NLI is not calculated for very small or very large power deviations, affected by measurement noise or system transients, respectively.

3 OVERVIEW OF LOCAL EMERGENCY CONTROLS

3.1 Overview of emergency controls

This section reviews previously developed emergency control schemes to provide a comparison with the new schemes developed in this paper, which are introduced in Section 4. The schemes reviewed here are all local while the ones developed in Section 4 are wide-area. All emergency control schemes are characterized by the following attributes:

1. Whether they are purely local or wide-area (global)
2. The control function and the device where it is applied
3. The triggering criterion initiating the emergency control, and
4. The reset criterion to terminate the emergency control action.

The schemes compared in this paper are summarized in Section 4.3 and the performance criteria for the comparison are discussed further below, in Section 5.

3.2 Scheme A: Emergency control using inverse tap changes (LIVES-restore)

This emergency control scheme does not require reactive support by IBGs and is included in the paper in order to show the improvement introduced with further reactive support by the IBGs.

Scheme A is based on LIVES-alarm signal and is a local emergency control against long-term voltage instability presented in [19]. The control consists of a series of reverse tap operations (in favor of the transmission voltage) at the transformer where the alarm was issued. The reverse tap operations stop (reset criterion) when a voltage stability condition is identified through an increase of transmission side voltage, or after a maximum number of reverse taps is reached. When the reset condition is satisfied, a LIVES-restore signal is issued and the LTC setpoint (center of the deadband) is decreased, so that it becomes equal to the measured distribution voltage at the time the LIVES-restore signal is issued, implementing in effect an indirect load curtailment by means of distribution voltage setpoint reduction. This method is entirely local within the substation, and does not require any communication with other substations.

3.3 Scheme B: LIVES-restore combined with IBG reactive support

In the presence of IBGs in the same distribution grid, Scheme A is modified as proposed in [6] by imposing a ramp on the IBG terminal voltage setpoint, resulting in a reactive power ramp from the inverters connected to the feeder on which the alarm was issued. The IBG terminal voltage ramp has a constant and slow rate so as to allow the LTC to restore distribution voltage within the modified deadband. The individual ramp is activated T_d seconds after the LIVES-restore signal has been issued, and stops either when the terminal voltage of the IBG reaches a maximum acceptable value V_{IBG}^{max}, or when the rated current of the inverter I^{lim} is reached.

After the LIVES-restore signal, normal LTC operation is restored but with the lowered deadband, thereby allowing the LIVES algorithm to continue monitoring long-term voltage stability. In this sense, this local emergency action can be seen as a closed-loop control. Namely, if instability is detected again a new round of corrective actions will be applied.

4 NEW GLOBAL EMERGENCY CONTROL SCHEMES

In this Section the new proposed wide-area protection schemes against voltage instability are presented.

4.1 Scheme C: Distributed restoration of transmission voltages

This approach is based on the method presented in [9], where the emergency control was triggered by a local indicator and applied in each distribution grid independently. A new, wide-area version of this method is further developed in this paper, and is summarized as follows.

The triggering signal for the countermeasures is global and is issued to all substations in the monitored area, as soon as two LIVES alarms are received in the area protected. Relying on two LIVES alarms avoids unduly reacting to a false alarm issued by a single distribution network. At the moment the alarm is received, in each distribution grid the voltage V_t on the transmission side of the distribution transformer is recorded into V_t^{min} while the voltage V_d on the distribution side is recorded as V_d^{max}.

Emergency control starts after a delay of τ_{db} seconds. The objective is to uplift V_t by means of emergency IBG reactive power support and keep it above V_t^{min} (hence, the term "transmission voltage restoration"). Once this is achieved, the IBG reactive powers are left at their current values. If V_t falls again below V_t^{min}, the IBGs resume their reactive power increase. The scheme is applied in each distribution grid independently, aiming to restore the voltage on the transmission side of its transformer. In parallel, the distribution transformer has its voltage setpoint decreased to V_d^{max} to avoid load power restoration, as already explained.

Fig. 2 shows graphically the actions taken, which can be summarized as follows:

1. the LTC deadband is decreased to [$V_d^{max} - \varepsilon \quad V_d^{max} + \varepsilon$], where ε is the original half-dead-band;

2. while $V_d < V_d^{max} - \varepsilon$ and $V_t < V_t^{min}$, the LTC remains idle, i.e. the transformer ratio r is not further decreased to support the distribution voltage, while IBGs inject reactive power. The opposite holds true if $V_d < V_d^{max} - \varepsilon$ but $V_t > V_t^{min}$, with IBGs no longer injecting reactive power and the transformer ratio r being allowed to decrease according to the standard LTC control logic. The motivation is to avoid impacting customer voltages while the transmission voltage V_t does not show an emergency situation;

3. similarly, if $V_d > V_d^{max} + \varepsilon$, the transformer ratio r is increased as usual (to bring V_d in the new LTC deadband). If $V_t < V_t^{min}$, the IBGs are again called to support the transmission voltage.

The emergency control is applied in each distribution grid independently and the stopping signal remains local, i.e. the restoration of the voltage on the transmission side of the transformer of each substation. Thus, all controls begin simultaneously, but each has its own termination condition.
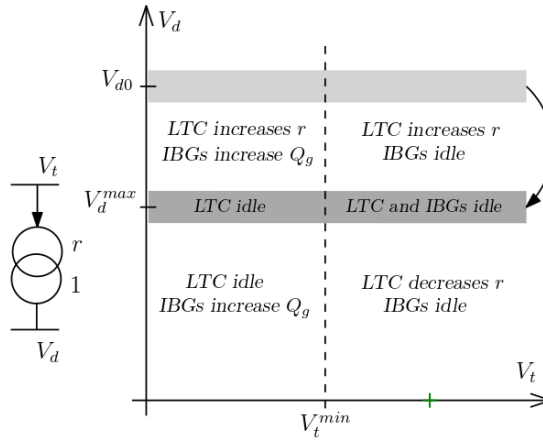

Fig. 2 Control logic of distributed transmission voltage restoration Scheme C. The arrow shows the decrease of the LTC voltage setpoint from V_{d0} to V_d^{max} at the time of alarm.

4.2 Scheme D: Voltage stability protection using NLI

The wide-area instability identification and control approach developed in this section uses the NLI instability monitoring presented in Section 2.2 at the EHV boundary buses of the importing area, which is considered prone to long-term voltage instability. Emergency control is activated simultaneously on all substations located in the monitored area either a few seconds (τ_1) after a single NLI alarm, or with a shorter delay (τ_2) after N successive NLI-alarms, N being the number of monitored boundary buses.

The emergency control presented here is similar to the local scheme described in Section 4.1 in terms of the control actions and the monitored variables, the difference being that it is activated by the wide-area NLI alarm signals in a uniform way across all involved substations of the monitored area. The protection system is reinstated when all monitored NLIs become positive, thereby indicating that the system has restored voltage stability.

It must be stressed that, after the initial alarm and during the emergency control actions, NLI is still calculated at the transmission buses of concern. When all NLIs have regained positive values, the emergency control phase is terminated after a predetermined time delay τ_3. Then, a restoration phase follows, which consists of the following steps in each feeder:

1. The reactive support ramp is stopped and reactive generation from IBGs remains constant;
2. LTC normal operation is resumed (in both directions) but with the new, decreased deadband;

NLI monitoring at the boundary buses remains active. If a new alarm is issued, the same emergency controls are applied. In this sense this control scheme can be considered as closed loop emergency control.

4.3 Summary

The main characteristics of the four emergency control schemes against voltage collapse A to D, already presented in Sections 3 and 4, are summarized in Table 1.

Table 1 Characteristics of emergency control schemes

Scheme	Alarm	Control	Reset
A	Local	Reverse LTC + V_{d0} reduction	$\Delta V_t > 0$
B	Local	Reverse LTC + V_{d0} reduction +IBG V ramp	ΔV_t>0 for reverse LTC, I^{max} for IBG V ramp
C	Global	V_{d0} reduction + IBG Q ramp	$V_t \geq V_t^{min}$
D	Global	V_{d0} reduction + IBG Q ramp	NLI>0

5   EMERGENCY CONTROL PERFORMANCE CRITERIA

The emergency control schemes reviewed above are avoiding voltage collapse by modifying LTC tap operation and distribution voltage setpoint, as well as by employing IBG reactive support. The reduction of the distribution system setpoint constitutes an indirect load power reduction. This function of reducing load consumption by voltage setpoint adjustment is common to all emergency control schemes considered in this paper.

As discussed in the Introduction, when combining with reactive support by the IBGs, care is taken that the reactive power injection by the IBGs does not counteract the desired load voltage reduction. To achieve this coordination, in all emergency control schemes the reactive support from the IBGs is applied through a slow reactive power ramp, with a slope that will allow the LTC to maintain the distribution voltage at the reduced value specified by the control scheme.

The amount of indirect load reduction applied to restore voltage stability is the first performance criterion used in this paper to assess and compare the performance of each emergency control scheme. Assuming that the loads can be represented by an exponential model, the Total Indirect Load Reduction (TILR) is quantified using the following formula:

$$\boldsymbol{TILR} = \sum_{i} (\boldsymbol{P_{o,i}}/V_{oi}^{\alpha})\left(V_{min,i}^{\alpha} - V_{fin,i}^{\alpha}\right) \tag{5}$$

where $\boldsymbol{P_{o,i}}$ and $\boldsymbol{V_{o,i}}$ are respectively the initial load power and voltage of the i-th load, while $\boldsymbol{V_{min,i}}$ and $\boldsymbol{V_{fin,i}}$ are respectively the lower limit of the LTC original deadband and the final load voltage (i.e. after a new long-term equilibrium is achieved). The sum extends over all loads with lowered LTC deadband. The exponent $\boldsymbol{\alpha}$ is the normalized sensitivity of load consumption to bus voltage.

Regarding the participation of IBGs in the reactive support, it is noted that this is subject to the constraints of maintaining acceptable voltage at the distribution feeder (between 95% and 105%), and also of respecting the maximum converter current limit $\boldsymbol{I_i^{max}}$ of each converter. Thus, IBGs have limited capability to offer reactive support.

The remaining capability of IBGs to provide reactive power support after the application of the emergency control, is the second performance criterion used in this paper. This capability is measured by the current availability percentage q_r, which is defined as the ratio of available converter current margin versus total nominal current:

$$q_r = \frac{\sum_{i=1}^{N}(I_i^{max} - I_i)}{\sum_i^{N} I_i^{max}} \tag{6}$$

where N is the total number of IBGs in the area monitored by the protection scheme, I_i is the injected IBG current after a new long-term equilibrium is achieved, and I_i^{max} is the IBG rated current (corresponding to its nominal voltage and apparent power). It is noted that the available control margin is limited also by the active current of the converter.

6   TEST SYSTEM, INSTABILITY SCENARIO AND MONITORING

6.1   Modified Nordic Test System

The test system used in this analysis is a modified version of the IEEE Nordic Test System detailed in [21] and operating at the insecure point A. The changes applied to the original version of the test system are the same as in [6] and concern the inclusion of approximately 970 MW of IBG production in the Central area at distribution level. The IBG production is modelled in an aggregate way in order to keep a simple – yet straightforward – approach for extracting clear and indicative conclusions. The system single-line diagram is depicted in Fig. 3.
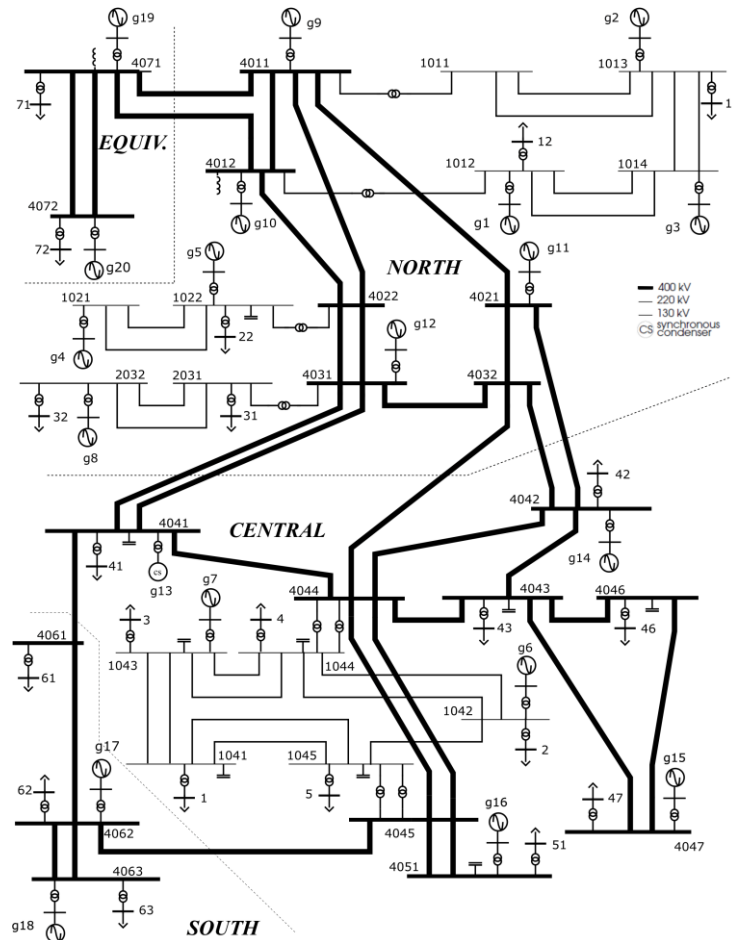

Fig. 3 IEEE Nordic Test System single-line diagram

As depicted in Fig. 4, the aggregate IBG is connected to each load bus of the Central area (bus with voltage V_{MV} in Fig. 4) through a dedicated feeder with impedance $R+jX$. The detailed data of the IBGs and loads of the modified test system are given in Table 2. The feeder data were taken from real wind farm feeders connected to the Hellenic transmission system and were scaled accordingly.

Moreover, in order to achieve the same initial power flow solution as that of operating point A in [21], all loads in the Central area had to be adjusted, as shown in the corresponding columns P_L and Q_L in Table 2.
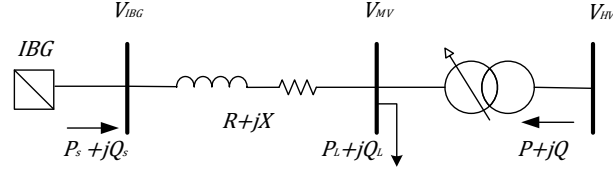

Fig. 4 IBG inclusion at distribution level (the system operates initially with Q_s=0)

In all simulations P_s remains constant (assuming maximum power tracking mode of the distributed generator) and the IBGs operate with UPF, except when emergency reactive support is activated, in which case a ramping reactive power setpoint is applied.

Table 2 IBG, feeder and load characteristics (pu values on 100 MVA base and transformer nominal voltages)

IBG Bus #	P_s (MW)	S_n (MVA)	P_{max} (MW)	P_L (MW)	Q_L (Mvar)	R (pu)	X (pu)
1	97.20	113.68	108.00	696.78	142.47	0.004413	0.060800
2	99.30	110.05	104.55	425.22	62.65	0.045050	0.091650
3	64.60	71.58	68.00	321.60	78.12	0.077986	0.147573
4	90.00	100.00	90.00	927.60	241.11	0.030800	0.139600
5	81.00	94.74	90.00	800.65	185.60	0.005296	0.072960
41	115.88	128.39	121.98	651.05	121.57	0.038614	0.078557
42	60.72	67.28	63.92	457.89	122.04	0.082964	0.156993
43	108.00	120.00	108.00	1005.1	241.58	0.025666	0.116333
46	87.48	102.32	97.20	787.11	206.65	0.004903	0.067555
47	92.70	102.72	97.58	188.82	36.11	0.048267	0.098196
51	69.70	77.31	73.44	866.53	252.07	0.072209	0.136642

6.2 Monitored area

In this test system, the importing area of Section 2.2 corresponds to the Central area, and the exporting area to the North one. The transfer corridor is formed by the transmission lines connecting the sending boundary buses 4021, 4031 and 4032 with the receiving boundary buses 4041, 4042, 4044. Each receiving boundary bus has a set of sending boundary buses as mentioned in Section 2.2, e.g. for bus 4042, K_{4042} = {4021,4032} and three NLIs for the receiving boundary buses can be computed in the system pre-contingency state.

6.3 Initiating disturbance

The simulated scenario is identical to the one presented in [21], i.e. a solid three-phase fault occurs at t=1s next to bus 4032 and is cleared after 5 cycles by disconnecting line 4032-4044. The disconnection of this circuit results in 4044 not being a boundary bus anymore, leaving two NLIs to be computed, at boundary buses 4041 and 4042. Unless otherwise specified, the system has been simulated

with the RAMSES software developed at the Univ. of Liège [22] and relying on the phasor-mode (or RMS) approximation. The default time step size is 10 ms.

In Fig. 5, the evolution of voltage at EHV buses 4042 and 4044, as well as the HV bus 1042 is shown. The system exhibits long-term voltage instability and eventually loses short-term equilibrium at 181 s due to generator angle instability.
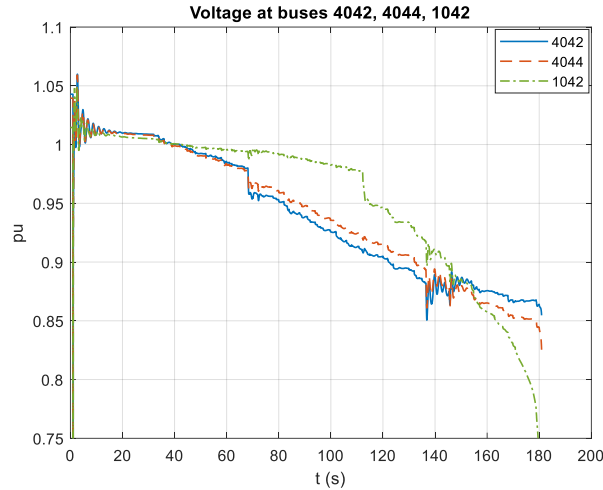

Fig. 5 Evolution of voltages at transmission buses 4042, 4044 and 1042

The long-term voltage instability onset is identified during the simulation by performing sensitivity analysis with the WPSTAB software of NTUA [6]. More specifically, the sensitivity of total reactive power generation Q_g with respect to individual reactive load consumptions is calculated at each bus, using the Jacobian matrix of the long-term system equilibrium equations [23]. It is noted that instability onset is slightly delayed in comparison to the simulation without IBG integration and is identified at time $t \approx 73s$, while system voltages are still above 0.95 pu, as seen in Fig. 5.

6.4 Instability monitoring performance

The performance of the voltage instability monitoring approaches of Section **2** is presented next. No emergency protection scheme is activated in these simulations and the alarm issue times are compared to the actual instability onset identified by sensitivities as discussed above.

6.4.1 LIVES instability monitoring

The LIVES monitoring scheme is assumed to be active on each distribution transformer of the system. Instability is identified in several substations, all located in the Central Area, verifying that this is the area prone to voltage instability. Table 3 shows the times when LIVES-alarm signals are issued as well as the corresponding transmission voltage magnitudes.

Table 3 LIVES-Alarms (no countermeasures)

$t(s)$	LIVES alarm at load bus #	Transmission side voltage (pu) at time of alarm
76	43	0.9654
78	1	0.9328
80	4	0.9267
80	46	0.9712
82	42	0.9464
85	5	0.9369

88	3	0.9365

As seen in Table 3, LIVES instability alarms are issued timely at seven buses, a few seconds after the actual long-term instability onset at t=73s, leaving ample time for actuating countermeasures.

6.4.2 NLI Monitoring

Since the Central Area is the monitored importing area, only NLIs at the area boundary buses 4041, 4042 are considered. Bus 4044 has lost its connection to the exporting area after the disconnection of line 4032-4044.

In Fig. 6 the evolution of the NLI at receiving boundary buses 4041 and 4042 is presented. It can be observed that at t=72s and t=74s NLIs at buses 4041 and 4042 respectively become negative. Thus, the NLI alarm practically coincides with the actual instability onset. This information can be used to restore system stability through system protection schemes.
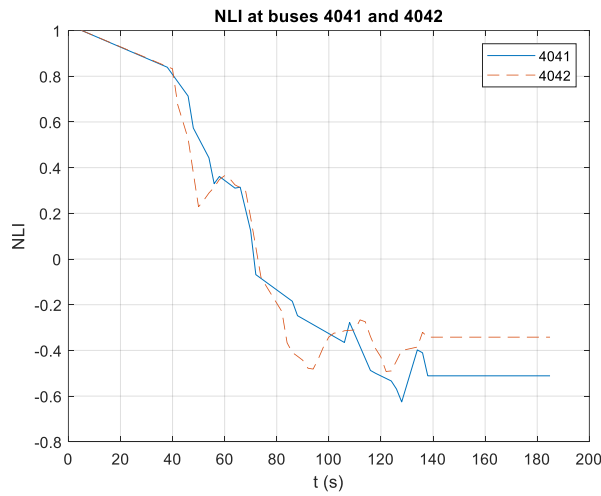

Fig. 6 Evolution of NLIs on remaining boundary buses 4041 and 4042

7 SIMULATION OF COUNTERMEASURES AND COMPARISON

7.1 Effect of IBG reactive support

Before proceeding to the simulation of countermeasure schemes, a preliminary assessment is made on the effect of the reactive support offered by the Central area IBGs, following the NLI alarm.

The reactive support from the IBGs is initiated after both NLIs at buses 4041 and 4042 become negative, while LTC transformers continue to operate normally without adjusting their deadbands. Fig. 7 shows the evolution of the transmission voltage at bus 1041, the distribution voltage at bus 1 and the LTC ratio. Nearly all Central area buses exhibit similar and unacceptable voltage profiles.
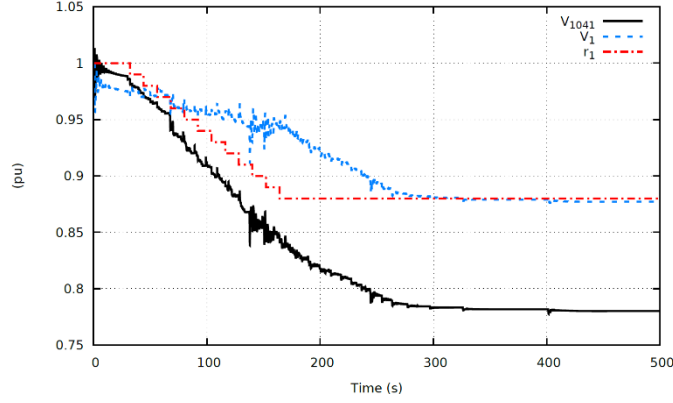
Fig. 7 Evolutions of transmission voltage (bus 1041), distribution voltage (bus 1) and LTC ratio. IBG reactive support, normal LTC operation

Fig. 7 shows that, while LTC transformers are operating normally, the system remains unstable despite the reactive support from all IBGs in the Central area. It is noted that the system does not actually collapse because LTCs reach their hard tap ratio limits r_{min}, thus stopping the instability mechanism of load restoration.

When acting alone, IBG reactive support slightly delays the instability but is not able to prevent it. This raises the need to apply more intrusive countermeasures against voltage instability, such as the ones presented in Section 4.

The parameter values of the necessary system protection schemes described in the previous sections are shown in Table 4.

Table 4 Parameters of System Protection Schemes

Local Schemes			Wide-area Schemes						
A & B			C			D			
T_d	V_{IBG}^{max}	$\Delta V_{IBG,ref}$	ΔQ	V_{IBG}^{max}	τ_{db}	τ_1	τ_2	τ_3	ΔQ
s	pu	pu/min	pu/5s	pu	s	s	s	s	pu/10s
10	1	0.06	0.05	1.1	3	10	5	5	0.05

7.2 Performance of countermeasure Schemes A and B.

The results shown in this section were produced using Quasi-Steady-State simulation [6]. Although this simulation method is an approximation, it has been compared to detailed simulation in [19], and it was found sufficient for demonstrating the performance of LIVES monitoring and emergency control scheme.

Table 5 lists the simulation results both with (Scheme B) and without reactive support by the IBGs (Scheme A). It is noteworthy that while the alarm signals of Table 5 follow the same pattern as in Table 3, no alarm is issued at buses 5 and 3, because the emergency control initiated at the buses of Table 5 relieves the system.

Table 5 System Protection Schemes A & B

$t(s)$	LIVES alarm at bus #	Transmission side voltage at time of alarm	Time of LIVES-restore signal (s)	V_d^{final} Scheme A (pu)	V_d^{final} Scheme B
76	43	0.9654	99	0.9483	0.9578
78	1	0.9328	103	0.9444	0.9541
80	4	0.9267	101	0.953	0.965
80	46	0.9712	105	0.9548	0.9723
82	42	0.9464	103	0.9382	0.9472

At first, only indirect load reduction is implemented (i.e. countermeasure Scheme A of Table 1) by means of reverse tap actions, as mentioned in Section 3.2, without reactive support from IBGs. In this case, the TILR calculated by means of Eq. (5) is equal to 159.57 MW, whereas the remaining control capability q_r is equal to 11.16%, due to the somewhat lowered distribution voltages giving rise to larger currents for the same active power dispatch by the IBGs. Inasmuch as no inherent load restoration mechanism is active this scheme provides a new stable equilibrium point.
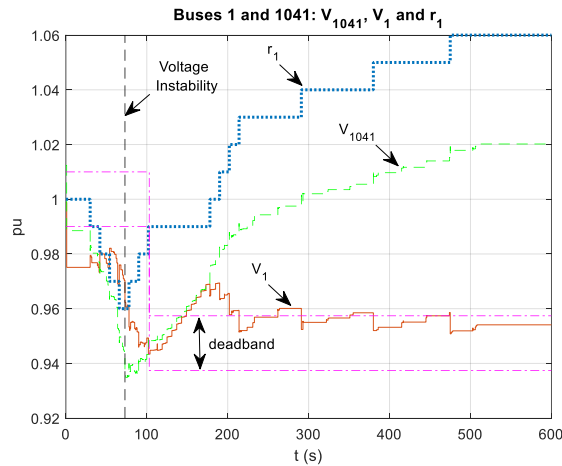

Fig. 8 Scheme B: Evolutions of transmission voltage (bus 1041), distribution voltage (bus 1) and LTC ratio

Fig. 8 shows the evolution of the transmission and distribution voltages of buses 1041 and 1, respectively, along with the corresponding LTC tap ratio when Scheme B is applied. It is quite obvious that a considerable enhancement of the transmission side voltage has been achieved with the reactive support ramp, while the distribution side voltage approaches the upper deadband limit as expected due to the reactive power increase by the IBGs, implying a smaller load reduction according to Eq. (5). From the voltage responses in Fig. 8 it can also be observed, that the IBG reactive power ramp rate is such that the LTC is able to bring the distribution voltage back to the adjusted deadband when an overshoot occurs. This implies that the LTC is able to suppress the load restoration mechanism that would have otherwise been re-activated due to the distribution voltage boost by the IBG emergency reactive power support.

A TILR of 114.21 MW is calculated in the case of Scheme B, due to the increased distribution voltages, clearly illustrating the potential that is offered by the distribution IBGs when reactive power support is provided during emergency conditions, while the remaining control capability of the IBGs is characterized by a q_r value of 7.56%. Reactive support is provided only by five distribution feeders in this case (see the first five alarms in Table 3), i.e. the ones where a LIVES-Alarm signal was issued.

7.3 Performance of countermeasure Scheme C

For consistency and comparison with the other protection schemes, the global alarm used in Scheme C is also based on LIVES-alarm signals. More precisely, a global alarm is sent to all distribution grids of the Central area once two successive LIVES-alarm are received from distribution grids (at t=78 s, see Table 3). After a delay τ_{db}, the actions detailed in Section 4.1 are taken simultaneously in all distribution grids of the Central area.

Fig. 9 shows the effect of the coordinated emergency control on the distribution grid connected to bus 1041. It shows the evolution of the transmission voltage (V_{1041}), the distribution voltage at bus 1 (V_1) as well as the transformer ratio (r_1).
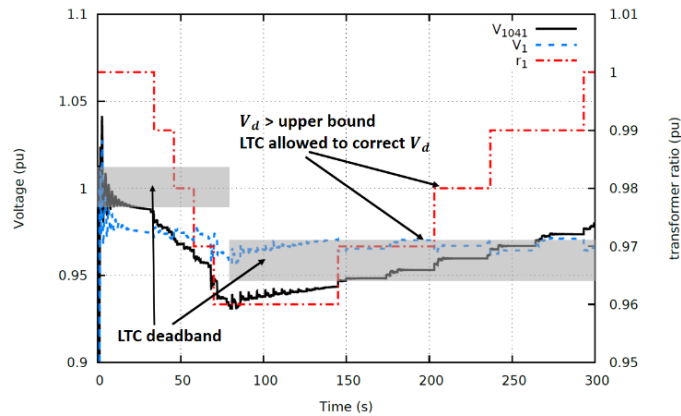

Fig. 9 Wide-area Scheme C: Responses of V_{1041}, V_1 and LTC ratio r_1

The global alarm is issued at $t = 78$ s, leading to $V_t^{min} = 0.9328$ pu at bus 1041 (see Table 5). After the delay τ_{db}, the LTC setpoint is decreased to the current value of V_1, which stops the decrease of V_{1041}. Under the effect of IBG reactive power injections, both V_1 and V_{1041} increase. Yet, when V_1 goes above the upper limit of the new deadband, the LTC is allowed to correct it, thereby avoiding load power restoration, in favour of transmission voltage restoration. It can be seen in Fig. 9 that the LTC ratio is increased four times after the alarm is issued, keeping V_1 below $V_d^{max} + \varepsilon$ and further increasing V_{1041}. As a result, the reactive power exported by the IBGs to the transmission grid is not accompanied by a load voltage increase, which would be counterproductive.
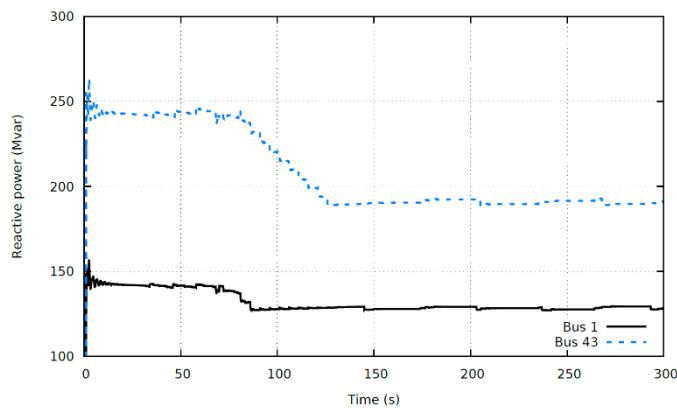

Fig. 10 Reactive power entering distribution network at bus 1 and 43

Finally, Fig. 10 shows the net reactive powers entering the distribution networks at buses 1 and 43, respectively. The decrease is due to the reactive power injection by IBGs; it stops either when $V_t > V_t^{min}$, or when the reactive power reserves are exhausted. The decrease of reactive power is

lower at bus 1 than at bus 43. An explanation can be that the value of V_t^{min} at bus 4043 (to which bus 43 is connected) is higher (see Table 3) at the time of the alarm, such that it requires more effort from IBGs to keep the voltage above V_t^{min}. Moreover, bus 4043 is at EHV transmission level (400 kV), while bus 1041 is at HV sub-transmission (130 kV); hence, the short-circuit power is significantly larger at the former bus, and voltage sensitivity to reactive power injection is lower, i.e. more effort is required for voltage restoration. Indeed, it is observed that the remaining reactive power reserves are mainly in IBGs connected to 130-kV buses, while the reactive power reserves of IBGs connected to the 400-kV buses 4041, 4042 and 4043 are all exhausted.

For this scheme, a TILR of 61.87 MW is observed, which is less than 1% of the total Central area load (see Table 2), while q_r is equal to 6.64%. This value of TILR is significantly smaller than the ones obtained with Schemes A and B, in which the additional reverse tap actions in favour of the transmission side reduce V_d with respect to its value at the time of the alarm, thereby imposing additional load curtailment. Yet, a comparison of the q_r values indicates that Scheme C leads to IBGs injecting more reactive power into the transmission system, in order to achieve the target voltage values V_t.

7.4 Performance of countermeasure Scheme D

The results of the wide-area protection Scheme D are given in this section with the utilized parameter set shown in Table 4. The reactive power ramp starts at 79 s, i.e. five seconds after the second NLI zero-crossing and it stops five seconds after both NLIs become positive again. Fig. 11 illustrates the evolution of transmission bus 1041 and distribution bus 1 voltages, as well as the corresponding tap ratio.
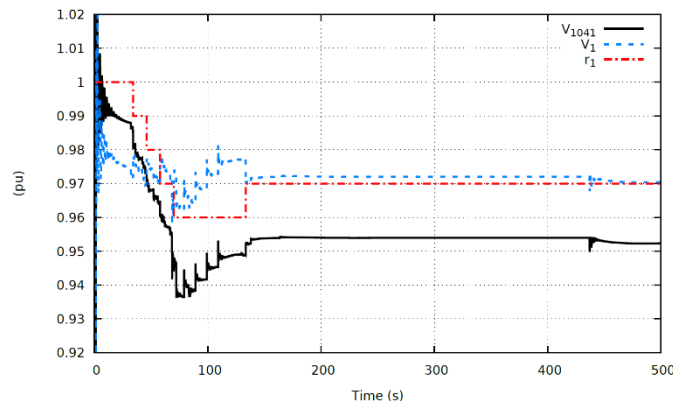

Fig. 11 Evolution of voltages bus 1041, bus 1 and branch 1-1041 LTC ratio with wide area emergency control based on NLIs

The TILR amounts to 99.95 MW, greater than the TILR of Scheme C but with less effort from IBGs, as indicated by a q_r value of 11.01%, significantly larger compared to Scheme C, as well as the other schemes. This leaves a larger margin for further support by IBGs if required.

7.5 NLI monitoring performance in case of further emergency

In this section the ability of NLI to identify a possible subsequent instability, so as to initiate a second application of the closed-loop Scheme D is demonstrated. Since, as shown above, the application of Scheme D was sufficient to restore stability, the simulation is extended in time with a subsequent further disturbance introduced at t=117 s, i.e., after the system has been stabilized. The second disturbance involves an increase of LTC distribution voltage setpoints at each load bus in the Central area simulating a maloperation of the local controllers. More specifically, the LTC setpoints increase at the specified time by a half LTC deadband. In this way, some distribution voltages fall below the new deadband, thus initiating LTCs operation to increase V_d and load power consumption.

16

As observed in Fig. 12, increasing the distribution voltages results in a load increase that the system cannot sustain. This gives rise to a new long-term instability and subsequent system collapse. The new instability onset is correctly identified by both NLIs at times between 230s and 250s, as seen in Fig. 13. Therefore, a new set of countermeasures can be applied to restore stability, which demonstrates the closed-loop ability of control Scheme D.
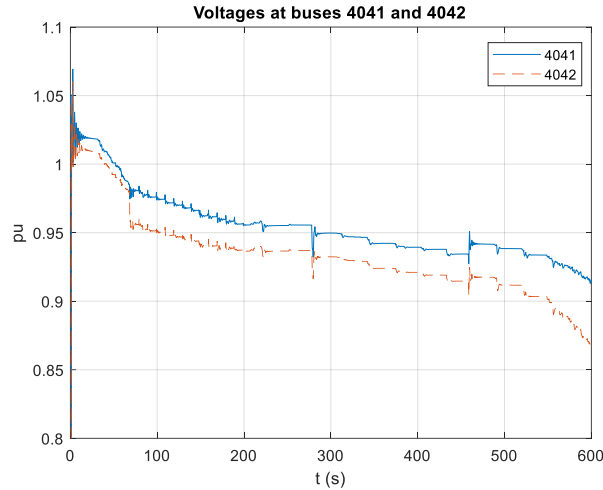

Fig. 12 Evolution of bus 4041 and 4042 voltages in response to a double disturbance (line outage followed by increased distribution volatges)
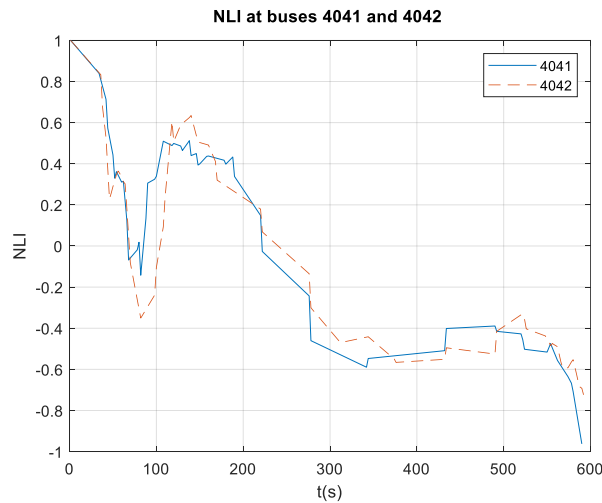

Fig. 13 Evolution of NLIs on boundary buses 4041 and 4042 in scenario with additional disturbance

7.6 Comparison

In the following Table 6 and Table 7, the results of all the presented emergency control schemes are summarized. Table 6 shows the TILR and q_r for each scheme. The initial (pre-disturbance) value of q_r is provided for comparison. As can be seen, the converters are already quite stressed due to the active power loading. Table 7 shows the final transmission voltages for all protection schemes.

From the results shown in these tables, it is deduced that Schemes C and D achieve superior overall performance, as the uniform reactive power provision leads to better distribution voltage profiles and smallest TILR. The advantage of Scheme D over C is the larger reactive power reserves left, since

it operates as a closed-loop control where IBGs simultaneously stop injecting reactive power when NLIs are positive again. This allows to keep sufficient reserve in order to face another possible event.

Table 6 Comparative results: reactive power provision, load reduction, and reactive reserves

Scheme	Total reactive power provision (MVAr)	Total Indirect Load Reduction (MW)	$q_{r,init}$(%)	$q_{r,final}$ (%)
A	-	159.57		11.16
B	266.82	114.21	11.59	7.56
C	369.57	61.87		6.64
D	217.62	99.95		11.01

Table 7 Comparative results: Final transmission bus voltages (pu)

Bus #	A	B	C	D
1041	0.9478	1.0202	1.0219	0.9524
1042	0.9928	1.0078	1.0186	0.9990
1043	0.9645	1.0242	1.032	0.9678
1044	0.9404	0.988	1.0006	0.9349
1045	0.9518	0.9939	1.01	0.9513
4041	0.9859	1.0094	1.03	0.9751
4042	0.9642	1.0073	1.0218	0.9495
4043	0.9728	1.0176	1.0288	0.9641
4046	0.9803	1.0238	1.0329	0.9730
4047	1.0175	1.0492	1.0574	1.011
4051	1.0297	1.0534	1.0675	1.031

It is clear that activating countermeasures simultaneously (Schemes C and D) improves the performance of the system with respect to cases where they are activated at separate times (as in Schemes A and B). Indeed, when acting at the same time, transmission buses are positively impacted by actions of adjacent buses, while when acting at different times, it is not always the case.

It is reminded though that Schemes C and D require a communication system and also a pre-defined set of distribution substation and IBG controls that need to be armed for action in the event of an alarm. However, the information flow in Scheme C is minimal since it merely involves broadcasting a triggering alarm signal.

It is noteworthy that in Scheme A, the reactive reserves are close to the ones of the wide-area Scheme D. This can be attributed to the reduced distribution voltages from the LIVES-restore processes, which gives rise to increased currents for the same amount of IBG active power production and thus reduces the reactive power reserves. This is a clear indication that the provision of emergency reactive support by the IBGs is desirable in all cases, provided that the rate of the IBG emergency reactive power provision is not faster than the LTC operation.

One disadvantage of protection Schemes B and C is that they both tend to exhaust the reactive power reserves of each distribution feeder called to support the transmission system. On the other hand, emergency control Scheme B is purely local and has no need for communication channels outside the substation and feeder.

8 CONCLUSIONS

This paper has compared existing to newly proposed emergency control schemes utilizing the control capabilities of IBGs in the distribution feeders in order to contain ongoing long-term voltage instability. The performance of the control schemes has been investigated for the IEEE Nordic test system on the IBGs located in all the substations of the central area, which is the one prone to voltage instability. For the simulated scenario there was no alarm issued in any of the other areas of the system. Thus, IBGs and emergency control schemes were not considered outside the central area.

Several key issues to achieve proper emergency controls involving distributed IBGs were highlighted in the paper:

1. The coordination of IBGs with other controls in the same distribution feeder is essential to provide the required service. As shown, the performance of the protection scheme depends on knowledge of feeder topology.
2. In particular, the reactive support ramp offered by the IBGs should be slow enough to allow the LTC to maintain the distribution voltage and avoid load restoration.
3. Online measurement-based voltage instability detection is crucial to allow effective emergency controls and avoid voltage collapse.
4. Harvesting a portion of the available IBG reactive power reserves reduces indirect load curtailment, as was clearly observed from the comparison of Scheme A to the other schemes.

The comparisons made in the paper showed that, even though in the examined test system the amount of reactive support available from the IBGs was not enough to correct the instability, if properly coordinated with LTC emergency controls that lower the distribution side voltage, it can significantly reduce the amount of indirectly reduced load to achieve stabilization. For instance, the amount of load reduction imposed by Scheme C is 62% smaller than the one imposed by Scheme A (62 MW compared to 159 MW).

It was also shown in the paper that applying simultaneous controls on all feeders in an area prone to voltage instability can improve the performance of emergency control. Two such wide-area control schemes were presented and compared: one with the goal to maintain transmission voltages above the value at the time of the alarm (Scheme C), and the other applying a closed-loop stability control based on NLI stability indicator (Scheme D). While the former achieves the minimum indirect load curtailment, it tends to draw more on IBG reactive power reserves, whereas the latter increases the indirect load reduction (by 38 MW) on the one hand, but on the other hand maintains a larger reactive control capability for subsequent support by IBGs in case of further emergency.

It should be stressed, that both Schemes C and D require communication infrastructure, in order to properly control each IBG to provide emergency reactive power support. This is certainly a challenging task, but one in line with the general tendency towards smart grids and distribution system automation.

Overall, applying the proposed methods to the test system demonstrated that measurement-based voltage stability monitoring and associated emergency controls involving LTCs and IBGs at the distribution level, are mature enough to be tested in practice for real-life applications.

9 REFERENCES

[1] N. Hatziargyriou, J. Milanovic, C. Rahmann, V. Ajjarapu, C. Cañizares, I. Erlich, D. Hill, I. Hiskens, I. Kamwa, P. Pourbeik, J. Sanchez-Gasca, A. Stankovic, T. Van Cutsem, V. Vittal, C. Vournas,

"Definition and Classification of Power System Stability – Revisited & Extended", IEEE Transactions on Power Systems. DOI 10.1109/TPWRS.2020.3041774.

[2] N. Hatziargyriou (chair) et al., "Contribution to Bulk System Control and Stability by Distributed Energy Resources connected at Distri-bution Network," IEEE PES Technical Report PES-TR22, Jan. 2017

[3] S. Corsi, "Voltage Control and Protection in Electrica Power Systems: From System Components to Wide-Area Control", Springer-Verlag, London 2015.

[4] H. Sun, Q. Guo, J. Qi, V. Ajjarapu, R. Bravo, J. Chow, Z. Li, R. Moghe, E. Nasr-Azadani, U. Tamrakar, G. N. Taranto, R. Tonkiski, G. Valverde, Q. Wu, G. Yang, "Review of Challenges and Research Opportunities for Voltage Control in Smart Grids", in IEEE Transactions on Power Systems, vol. 34, no. 4, pp. 2790-2801. DOI: 10.1109/TPWRS.2019.2897948

[5] Y. Li, L. Fu, K. Meng, Z. Y. Dong, "Assessment and enhancement of Static Voltage Stability With Inverter-Based Generators", IEEE Transactions on Power Systems, vol. 36, no. 3, pp. 2737-2740, May 2021.

[6] P. Mandoulidis, T. Souxes, and C. Vournas, "Impact of Converter Interfaced Generators on Power System Long-Term Voltage Stability Monitoring and Control", Electric Power Systems Research, vol. 199, October 2021. DOI https://doi.org/10.1016/j.epsr.2021.107438

[7] P. Li, H. Ji, C. Wang, J. Zhao, G. Song, F. Ding, J. Wu, "Coordinated Control Method of Voltage and Reactive Power for Active Distribution Networks Based on Soft Open Point," *in IEEE Transactions on Sustainable Energy*, vol. 8, no. 4, pp. 1430-1442, Oct. 2017. DOI: 10.1109/TSTE.2017.2686009

[8] P. Aristidou, G. Valverde, T. Van Cutsem, "Contribution of Distribution Network Control to Voltage Stability: A Case Study", IEEE Trans. on Smart Grid, vol. 8, no. 1, pp. 106-116, Jan. 2017.

[9] L.D.P. Ospina, T. Van Cutsem, "Emergency support of transmission voltages by active distribution networks: a non-intrusive scheme", IEEE Trans. on Power Systems, 2020 Early Access Article, DOI 10.1109/TPWRS.2020.3027949I.

[10] L.D.P. Ospina, T. Van Cutsem, "Power factor improvement by active distribution networks during voltage emergency situations", Electric Power Systems Research, vol. 189, December 2020.

[11] M. Glavic, T. Van Cutsem, "A short Survey of Methods for Voltage Instability Detection", Proc. IEEE PES General Meeting, Detroit (USA), 2011.

[12] F. Hu, K. Sun, A. Del Rosso, E, Farantatos, N. B. Bhat, Measurement-Based Real-Time Voltage Stability Monitoring for Load Areas, IEEE Trans. on Power Systems, Vol. 31, No. 4, 2016.

[13] Y. Wang, I. R. Pordanjani, W. Li, W. Xu, T. Chen, E. Vaahedi, J. Gurney, "Voltage stability monitoring based on the concept of coupled single-port circuit", IEEE Trans. on Power Systems, Vol. 26, No. 4, 2011.

[14] K. Uhlen, T. D. Duong, D. Karlsen, Use of Voltage Stability Assessment and Transient Stability Assessment Tools in Grid Operations, Springer, 2021.

[15] L. Robitzky, "Analysis of long-term voltage stability in electric power systems under consideration of active distribution networks and novel emergency control systems", Ph.D. dissertation, Fakultät für Elektrotechnik und Informationstechnik, Techn. Uni. Dortmund, Dortmund, Germany, 2018.

[16] S. Corsi, G. N. Taranto, "A Real-Time Voltage Instability Identification Algorithm Based on Local Phasor Measurements", *IEEE Transactions on Power Systems*, vol. 23, no. 3, August 2008.

[17] C. D. Vournas, T. Van Cutsem "Local Identification of Voltage Emergency Situations," IEEE Trans. on Power Systems, vol. 23, no. 3, pp. 1239–1248, Aug. 2008.

[18] T. Weckesser, L. Papangelis, C.D. Vournas, and T. Van Cutsem, "Local identification of voltage instability from load tap changer response", Sustainable Energy, Grids and Networks, vol.9, pp.95-103, 2017.

[19] C. D. Vournas, C. Lambrou, M. Kanatas, "Application of Local Autonomous Protection Against Voltage Instability to IEEE Test System", IEEE Trans. on Power Systems, vol.31, no. 4, pp. 3300–3308, Jul. 2016.

[20] C. D. Vournas, C. Lambrou, P. Mandoulidis, "Voltage Stability Monitoring from a Transmission Bus PMU", IEEE Trans. on Power Systems, Vol. 32, no. 4, pp. 3266 – 3274, May 2017.

[21] T. Van Cutsem, M. Glavic, W. Rosehart, C. Canizares, M. Kanatas, L. Lima, F. Milano, L. Papangelis, R. A. Ramos, J. A. dos Santos, B. Tamimi, G. Taranto, and C. Vournas, "Test Systems for Voltage Stability Studies", IEEE Trans. on Power Systems, vol. 35, no. 5, pp. 4078-4087, Sept 2020.

[22] P. Aristidou, D. Fabozzi, and T. Van Cutsem, "Dynamic simulation of large-scale power systems using a parallel Schur-complement-based decomposition method," IEEE Trans. on Parallel and Distributed Systems, vol. 25, no. 10, pp. 2561–2570, Oct 2014.

[23] T. Van Cutsem, C. Vournas, "Voltage Stability of Electric Power Systems", Norwell MA: Kluwer 1998, Springer 2008.